Carcinogenesis vol.27 no.8 pp.1558–1566, 2006
doi:10.1093/carcin/bgl007
Advance Access publication March 14, 2006

Association of gene expression with sequential proliferation, differentiation and tumor formation in murine skin

Katie Ridd, Shu-Dong Zhang, Richard E.Edwards, Reginald Davies, Peter Greaves, Alison Wolfreys[1], Andrew G.Smith and Timothy W.Gant*

MRC Toxicology Unit, Hodgkin Building Lancaster Road, PO BOX 138 University of Leicester, Leicester, LE1 9HN, UK and [1]Safety and Environmental Assurance Centre, Unilever, Colworth, Sharnbrook, Bedfordshire, MK44 1LQ, UK

*To whom correspondence should be addressed: Tel: +0116 252 5579; Fax: +0116 252 5616;
Email: twg1@le.ac.uk

Differential gene expression in two established initiation and promotion skin carcinogenesis models during promotion and tumor formation was determined by microarray technology with the purpose of distinguishing the genes more associated with neoplastic transformation from those linked with proliferation and differentiation. The first model utilized dimethylbenz[a]anthracene initiation and 12-*O*-tetradecanoylphorbol 13-acetate (TPA) promotion in the FVB/N mouse, and the second TPA promotion of the Tg.Ac mouse, which is endogenously initiated by virtue of an activated *Ha-ras* transgene. Comparison of gene expression profiles across the two models identified genes whose altered expression was associated with papilloma formation rather than TPA-induced proliferation and differentiation. DMBA suppressed TPA-induced differentiation which allowed identification of those genes associated more specifically with differentiation rather than proliferation. EASE (Expression Analysis Systemic Explorer) indicated a correlation between muscle-associated genes and skin differentiation, whereas genes involved with protein biosynthesis were strongly correlated with proliferation. For verification the altered expression of selected genes were confirmed by RT–PCR; *Carbonic anhydrase 2*, *Thioredoxin 1* and *Glutathione S-transferase omega 1* associated with papilloma formation and *Enolase 3*, *Cystatin β* and *Filaggrin* associated with TPA-induced proliferation and differentiation. *In situ* analysis located the papillomas *Glutathione S-transferase omega 1* expression to the proliferating areas of the papillomas. Thus we have identified profiles of differential gene expression associated with the tumorigenesis and promotion stages for skin carcinogenesis in the mouse.

Abbreviations: *Car2*, *Carbonic anhydrase 2*; *Cryab*, *aβ Crystallin*; *Cstb, Cystatin beta*; DMBA, dimethylbenz[a]anthracene; *eno3*, *Enolase 3*; EASE, Expression Analysis Systemic Explorer; EST, Expressed Sequence Tag; *Flg*; *Filaggrin*; Gst, Glutathione S-transferase; *Gsto1*, *Glutathione S-transferase omega 1*; *Inv*, *Involucrin*; RT–PCR, real time-PCR; TPA, 12-*O*-tetradecanoylphorbol 13-acetate; *Txn1, Thioredoxin 1*; T, TPA-treated; DT, DMBA and TPA-treated; D, DMBA treated.

Introduction

Murine models of skin carcinogenesis require an activating mutagenic event followed by multiple applications of an agent that induces clonal expansion (promotion) of the mutated cells to form tumors. Two mouse models were utilized that are widely used to study the molecular mechanisms of initiation and promotion in skin carcinogenesis. In the first, a single dose of carcinogen is followed by multiple doses of a promoting agent (1,2). In the second model, the Tg.Ac mouse carries an activated *Ha-ras* transgene, and requires only promotion to form papillomas (3). The papillomas that develop in both models are histopathologically similar. The phorbol ester 12-*O*-tetradecanoylphorbol 13-acetate (TPA) acts as an efficient promoting agent in these models by inducing homogeneous proliferation and differentiation of mouse skin cells, some of which are the progenitors for papillomas (3–5). Cells that are not initiated proliferate and differentiate when affected by TPA but upon TPA withdrawal do not progress to unregulated division (3,6). There is therefore a pathologically distinct phase of proliferation and differentiation prior to the formation of papillomas (3). This response to promotion results in the differential expression of many genes within the initiated cells prior to papilloma formation (7,8). It is not clear whether these alterations are necessary for the formation of papillomas or associated with proliferation and differentiation only.

Microarray technology has greatly facilitated the study of differential gene expression and allowed large-scale determination of gene expression changes associated with tissue changes and tumor formation. In the skin, microarrays have previously been used to study the basal gene expression of mouse strains that are sensitive or resistant to skin carcinogenesis (9), and to examine differential gene expressions associated with the effects of UV irradiation on keratinocyte wounding (10). Several studies have examined genes differentially expressed in C57BL/6 and NMRI mouse skin in response to a single dose of TPA and in isolated cells from Tg.Ac mice treated with multiple doses of TPA (7,8,11,12). The purpose of this study was to characterize differential gene expression in murine skin carcinogenesis models by comparing FVB/N and Tg.Ac mouse skin prior to, and after, the formation of papillomas. For the classic initiator and promoter protocol using dimethylbenz[a]anthracene (DMBA) initiation and

TPA promotion (13) FVB/N mice were chosen as these have the same genetic background as Tg.Ac mice. Tg.Ac mice require only promotion with TPA. Further analysis was applied to classify whether gene changes were associated with either the tumor formation or the hyperproliferative and differentiation response to promotion by TPA. By comparing common gene expression changes in the two models of skin carcinogenesis we sought to demonstrate the association of these genes with tumor formation in the skin.

Materials and methods

Animals

Female FVB/N and Tg.Ac (hemizygotes) mice 3–5 weeks of age were purchased from Harlan UK and Taconic UK, respectively. The mice were contained in an isolator and maintained at 19°C with 50% relative humidity and a 12-h light–dark cycle. Following a 1 week acclimatization period the dorsal skin of the mice was shaved using clippers (approximately 8 cm^2 area) 2 days prior to commencing topical treatments. FVB/N mice (five per group) were treated with DMBA (10 μg/200 μl in acetone) or vehicle control 1 week before promotion with TPA. FVB/N and Tg.Ac mice (five per group) were treated with TPA (2.5 μg/200 μl in acetone) twice a week for up to 14 weeks; control mice received acetone. All chemicals were applied topically using a pipette. Mice were shaved and examined weekly for the presence of papillomas. At each time point the mice were killed by cervical dislocation and the dorsal skin removed, a representative portion was fixed in 10% neutral buffered formalin for 1 week and processed conventionally, sectioned and stained with haematoxylin and eosin. The remainder of the tissue was snap frozen in liquid nitrogen.

Proliferation measured by PCNA immunohistochemistry

Mouse skin sections (5 μm) were cut, dewaxed and taken to water. Antigen retrieval was performed by microwaving at 700 W for 20 min in 0.01 M citrate pH 6. The primary antibody to Proliferating Cell Nuclear Antigen (Novocastra, Newcastle upon Tyne, UK, NCL-PCNA) was used at a dilution of 1:100 and applied to the sections for 3 h at room temperature. Serial control sections were treated similarly, with the primary antibody replaced by negative control mouse IgG2a (DAKO, Cambridgeshire, UK X0943). The primary antibody was detected using a peroxidase-labelled anti-IgG2a antibody (Serotec, Oxford, UK, STAR82P). The peroxidase was detected using 3,3-diaminobenzidine tetrahydrochloride, with the sections lightly counterstained with haematoxylin. The number of cells staining positive for PCNA were counted in five different fields for each section. The average number of stained cells per field was calculated for each treatment. Statistical significance was calculated using a two-tailed unpaired Student's *t*-test.

RNA extraction

Approximately 500 mg of tissue was homogenized on ice in Tri reagent (2 ml) using an Ultraturrax blender and chloroform/isopropanol extraction was performed twice. During the second round of extraction an extra chloroform extraction step was added to ensure the RNA was free from lipophilic contaminants.

Microarrays

To construct the cDNA microarrays, Expressed Sequence Tag (EST) clones were obtained from the IMAGE collection (MRC Geneservice, Cambridge, UK) and amplified by PCR. The DNA was printed in betaine (14) onto poly-L-lysine coated slides. Prior to use the slides were baked for 2 h at 80°C, washed in two changes of 0.2% SDS and two changes of water before being denatured by baking at 100°C for 2 min. Labelling and hybridization reactions were carried out as previously described (15) except that Microcon YM30 columns (Millipore, Massachusetts, USA) were used to purify the final reaction products and the slides were prehybridized as previously described (16). In some experiments repeat hybridizations were carried out with reversal of the fluorescent dyes. Where the amount of RNA was limiting, 5 μg of RNA was labelled using Genisphere 3DNA® array 350™ labelling kits (InterVascular, Cedex, France) following the manufacturer's instructions. After hybridization for at least 16 h at 42°C in a 50% formamide buffer the slides were washed as described by (15) and the fluorescence was measured using GenePix version 3.0 software (Axon Instruments, CA, USA). Microarray data are available on Arrayexpress (http://www.ebi.ac.uk/arrayexpress/) using the accession numbers E-MEXP-188, A-MEXP-98, A-MEXP-99, A-MEXP-100 and A-MEXP-101.

Samples were hybridized to microarrays as follows: (i) TPA-treated only (T) against DMBA/TPA (DT) with the purpose to identify tumor-associated genes. This comparison was designed to cancel out any effect of proliferation, differentiation or TPA exposure; (ii) DMBA only (D) against DMBA/TPA (DT) to identify those genes both tumor, proliferation- and differentiation-associated; and (iii) Tg.Ac control against Tg.Ac TPA-treated. This combination was designed to confirm the data obtained from the FVB/N DT mice in a different model with a different initiation protocol.

Normalization and statistical analysis

Median pixel–fluorescent intensity data from each array feature were collected and the local background was subtracted prior to analysis. Data were normalized by a global normalization procedure. Background was not subtracted as this had been established to have a detrimental effect on the data (Zhang and Gant, personal communication). Fluorescence data from each array feature were retained in the data set if positive with respect to the background. A threshold cut-off was not used except where there existed fluorescent data in only one channel. These data were retained in the data set if the intensity of fluorescence in the single channel was greater than 40% of the mean channel value. After normalization, the ratio of hybridization between the control and treated samples (where there existed fluorescent values for both channels) was calculated and statistical analysis of the results performed according to the methods described by (17). All genes that were significantly altered ($P \leq 0.05$) in expression in at least one sample of the time course were clustered using hierarchical clustering (Cluster 3, University of Tokyo, Human Genome Centre). EASE (Expression Analysis Systemic Explorer) analysis was performed using bootstrapping with 10 000 iterations on the individual gene sets associated with the pathological changes (18).

Real time–PCR (RT–PCR)

RNA (400 ng) was reverse-transcribed using Superscript II (Invitrogen, Paisley, UK) and the resulting cDNA was used for amplification with SYBR® green mastermix (Applied Biosystems, Warrington, UK). Reactions were carried out on an ABI PRISM® 7700 RT–PCR machine using optimized primers. Primers for RT–PCR were designed using Primer Express® software v2.0 (Applied Biosystems, Warrington, UK). The sequences used were: *Car2*: forward, CAAGCACAACGGACCAGAGAA, reverse, GGGCAGTTGCTGTGTCAATGT; *Cryab*: forward CGGAGGAACTCAAAGTCAAGGT, reverse ATCCGGTACTTCCTGTGGAACTC; *Cstb*: forward, CCGTGCTACCCCGACTACTG, reverse, CAAACTTCTGATTTTCTTTCGATTCA; *Eno3*: forward, GCTCCGTGACGGAGTCCAT, reverse, AGCGGTGGCTCACCATCA; *Flg:* forward, AACACTGAGCAAAGAAGAGCTGAA, reverse, CAGCGAAATCTAGTTTGTCATCGT; *Gsto1*, forward, CAGCGACTGGAAGCATTGG, reverse, CCGCCATCCAGAGCTTGA; *Txn1*, forward, TTCCTTGAAGTGGACGTGGAT, reverse, CTCACCTTTTGACCCCTTTTTATAA and *Inv,* forward, GAGCGTGAAGGTTATCAAGGA, reverse, TGCTGCTGCTTCTCTGTAGTG. The expression level of the gene of interest was normalized to that of *Cyclophilin A* in all samples. Statistical significance of the data was assessed by two-tailed *t*-test assuming unequal variance.

In situ hybridization

A plasmid containing a *Gsto1* (Accession number AV006756) insert was used to make a single stranded RNA probe labelled with biotin by incorporation of biotin-16-UTP (Roche, Penzberg, Germany). The reactions were purified using Microcon YM30 columns (Millipore, MA, USA) and alkaline digested with an equal volume of 100 mM sodium carbonate pH 10.2 for 71 min at 60°C. Following digestion, probes were neutralized with an equal volume of 0.2 mM sodium acetate, 1% glacial acetic acid (v/v), 10 mM dithiothreitol and precipitated overnight with sodium acetate and ethanol at −20°C.

An ELF® 97mRNA In Situ Hybridization kit (Invitrogen, Paisley, UK) was used to detect expression in paraffin-embedded skin sections (4 μm) on 3-aminopropyltriethoxysilane (APES)-coated slides. The manufacturer's instructions were followed for section preparation prior to, and after hybridization of the probe (10 ng), or no probe negative control. Prehybridization and hybridization conditions were as described for microarray experiments. Fluorescence was visualized using an Axioskop fluorescence microscope (Zeiss, Germany) and pictures were taken using a ProgRes C14 camera (Jenoptik, Jena, Germany).

Results

Papilloma formation and pathology

Papillomas were induced in DMBA-initiated FVB/N mice and Tg.Ac mice when promoted with TPA (Figure 1A). Both strains developed papillomas by 8 weeks after the commencement of promotion and all FVB/N mice were terminated by 14 weeks due to high papilloma burden. Papilloma

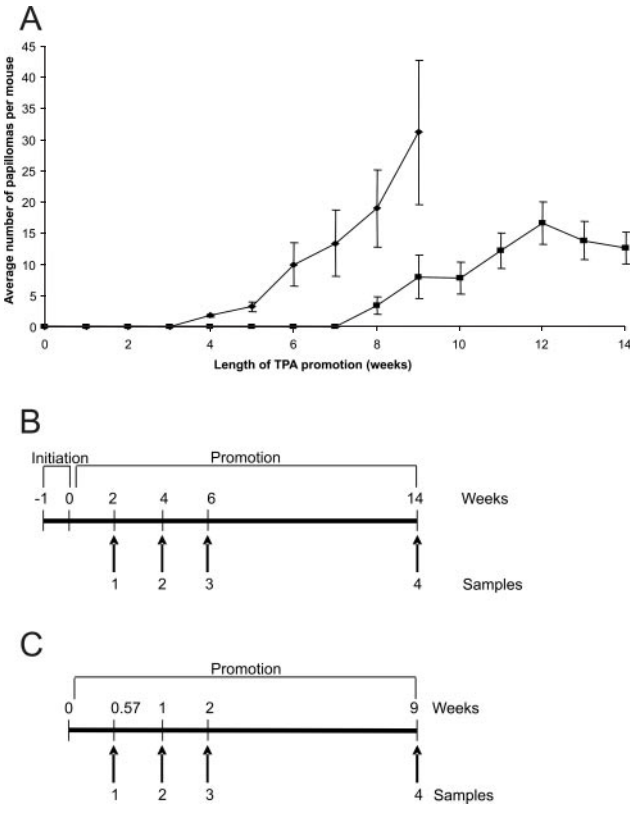

Fig. 1. Tumor latency and sample collection for FVB/N and Tg.Ac mice. FVB/N mice were initiated with DMBA (10 μg) 1 week prior to commencing TPA treatment. (**A**) Both FVB/N (rectangles) and Tg.Ac mice (diamonds) were treated with TPA (2.5 μg) twice weekly. Papillomas were counted at weekly intervals, five mice per strain and results are means ± SEM. (**B**) Following initiation of FVB/N mice at –1 week promotion began at week 0 and continued twice weekly for up to 14 weeks. Mouse skin was analysed for gene expression after 2, 4, 6 and 14 weeks of TPA treatment which corresponded to time points 1, 2, 3 and 4, respectively. (**C**) Promotion of Tg.Ac mice began at 0 weeks and continued twice weekly for up to 9 weeks. Mouse skin was analysed for changes in gene expression after 0.57, 1, 2 and 9 weeks of TPA promotion which corresponded to time points 1, 2, 3 and 4, respectively.

development occurred much faster in Tg.Ac mice and with a higher multiplicity leading to their termination after 9 weeks of promotion. Papillomas only formed in FVB/N mice that were both initiated and promoted (Figure 1A) as expected. Despite the altered latency and tumor burden very similar well-differentiated tumors were generated in both strains of mice. Due to the difference in papilloma latency time between the Tg.Ac and FVB/N, mice skin was isolated at different times in the two strains prior to the formation of papillomas. The time points were compared with each other by reference to papilloma formation rather than by absolute time from the commencement of promotion. Therefore, the Tg.Ac and FVB/N skin isolated 4 days and 2 weeks, respectively after commencing promotion were comparable in terms of length of time prior to papilloma formation. This was also true for Tg.Ac mice skin isolated after 1, 2 and 9 weeks and FVB/N skin isolated after 4, 6 and 14 weeks of promotion. The timescale of the sample collection for FVB/N is shown in Figure 1B and for Tg.Ac in Figure 1C. The histopathological changes in the skin over the time period can be seen in Figure 2. Mice treated with TPA showed a proliferative response demonstrated by an increase in epidermal thickness (Figure 2B to D) and an increase in the number of cells stained positive for PCNA (Figure 2L). The increase in the layers of flattened cells (arrows) containing keratohyaline granules in these skins also suggested a differentiation response to TPA (Figure 2B inset). The proliferative response to TPA was greater at 2 weeks in those mice initiated with DMBA prior to TPA treatment compared with TPA treatment alone, and similar at both 4 and 6 weeks (Figure 2L). Though proliferation was greater in the mice initiated with DMBA prior to TPA treatment, than in TPA alone, at 2 weeks the extent of differentiation was not as marked (Figure 2E inset). This DMBA mediated decrease in differentiation response to TPA was confirmed by *Involucrin* (Figure 2M) and *Filaggrin* (Figure 3B) expression which are both markers of keratinocyte terminal differentiation (19,20). Expression of these genes was reduced in the skin of mice initiated with DMBA prior to TPA treatment compared with those that received TPA alone. The TPA-only treated Tg.Ac and FVB/N mice showed similar proliferation responses (Figure 2I to K and Figure B to D). This was also true at the 14 (FVBN) and 9 week (Tg.Ac) time points when papillomas were present (Figure 2L).

Genomic analysis

In non-transgenic mice TPA treatment without prior initiation induced proliferation and differentiation, but did not lead to papilloma formation (Figure 1 and 2). Therefore, a microarray analysis of FVB/N mouse skin that had been initiated with DMBA and promoted with TPA would be complicated by gene expression effects caused either by the TPA directly or by the proliferative and differentiation response in the keratinocytes. To identify these changes two different microarray comparisons were made using FVB/N mouse skin. In the first comparison TPA-promoted skin (T) was compared with DMBA-initiated and TPA-promoted skin (DT). This comparison was designed to cancel out the effects of TPA exposure and so reveal those genes more closely associated with tumor formation. In fact as illustrated in Figure 2 the comparison cannot be absolute as DMBA had the effect of reducing the differentiating response of keratinocytes to TPA determined by *Filaggrin* (Figure 3B) and *Involucrin* (Figure 2M) expression. The second comparison was made between DMBA-initiated skin (D) and skin that was both DMBA-initiated and TPA-promoted (DT). This comparison generated a mixed response where gene expression changes could be associated with tumor formation, proliferation, differentiation or TPA exposure. For further discernment of gene designation, comparison was also made with the Tg.Ac experiment, where the gene expression responses to differentiation and tumorigenesis should be similar to FVB/N mice. In addition, in this experiment, we took a 4 day sample where direct responses to TPA may be more pronounced.

Genes were chosen for inclusion in Figure 3 if there was at least one time point where a gene showed a differential expression with a significance of $P \leq 0.05$. In total this gave 617 genes for multivariate analysis. The significance criterion used is relatively low with a potentially larger than desirable false positive rate. However, because of the nature of the experimental comparison this was the optimal method for selecting the genes to go forward for analysis. After selection of the genes various methods of grouping were tried including self-organizing maps and principal components analysis. However, in common with many analyses of this nature, hierarchical clustering with complete linkage was found to yield the

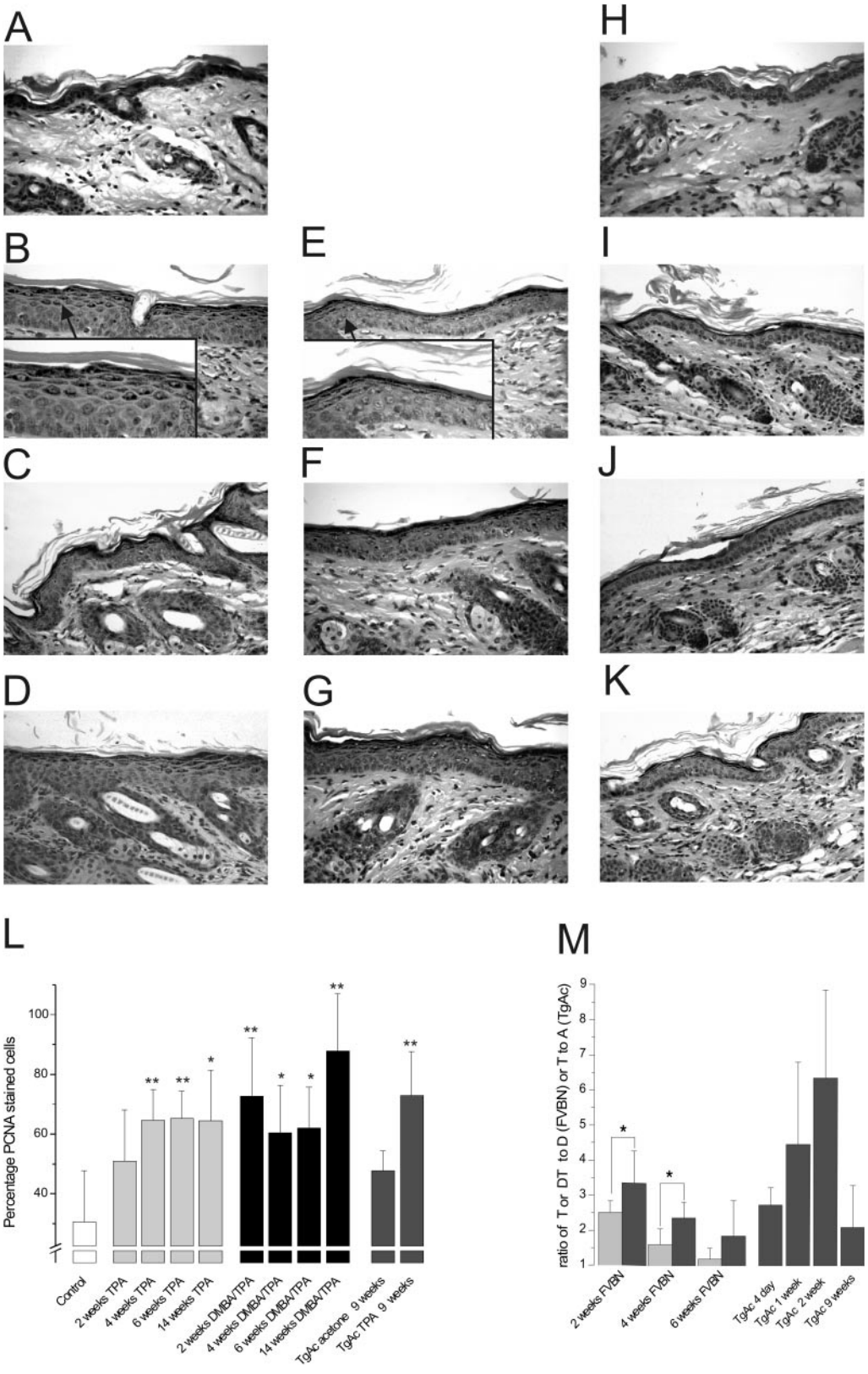

Fig. 2. Pathological responses to promotion and initiation and promotion in mouse skin. (**A**) Normal FVB/N mouse skin; (**B**) after 2 weeks; (**C**) 4 weeks; and (**D**) 6 weeks TPA promotion. Arrow and insert show differentiated, keratohyaline-containing cells. (**E**)–(**G**) are the pathological responses to DMBA initiation and subsequent TPA promotion at the same time points as (B)–(D), respectively. (**H**) Normal Tg.Ac skin and then at (**I**) 4 days, (**J**) 1 week and (**K**) 2 weeks promotion with TPA. (**L**) FVB/N mouse skin sections were stained with an antibody for PCNA. The number of PCNA positive epidermal cells was counted in five separate fields for each section with five different sections per designated treatment and time point. Means ± SD, *t*-tests were carried out between control and treated skin $^{*}P \leq 0.05$, $^{**}P \leq 0.01$. (**M**) RT–PCR analysis of *Involucrin* expression to confirm the altered differentiation with prior DMBA(D) treatment in response to TPA(T). Light grey, D/DT; dark grey D/T; $^{*}P \leq 0.05$ for differences between D/DT and D/T as indicated on the figure.

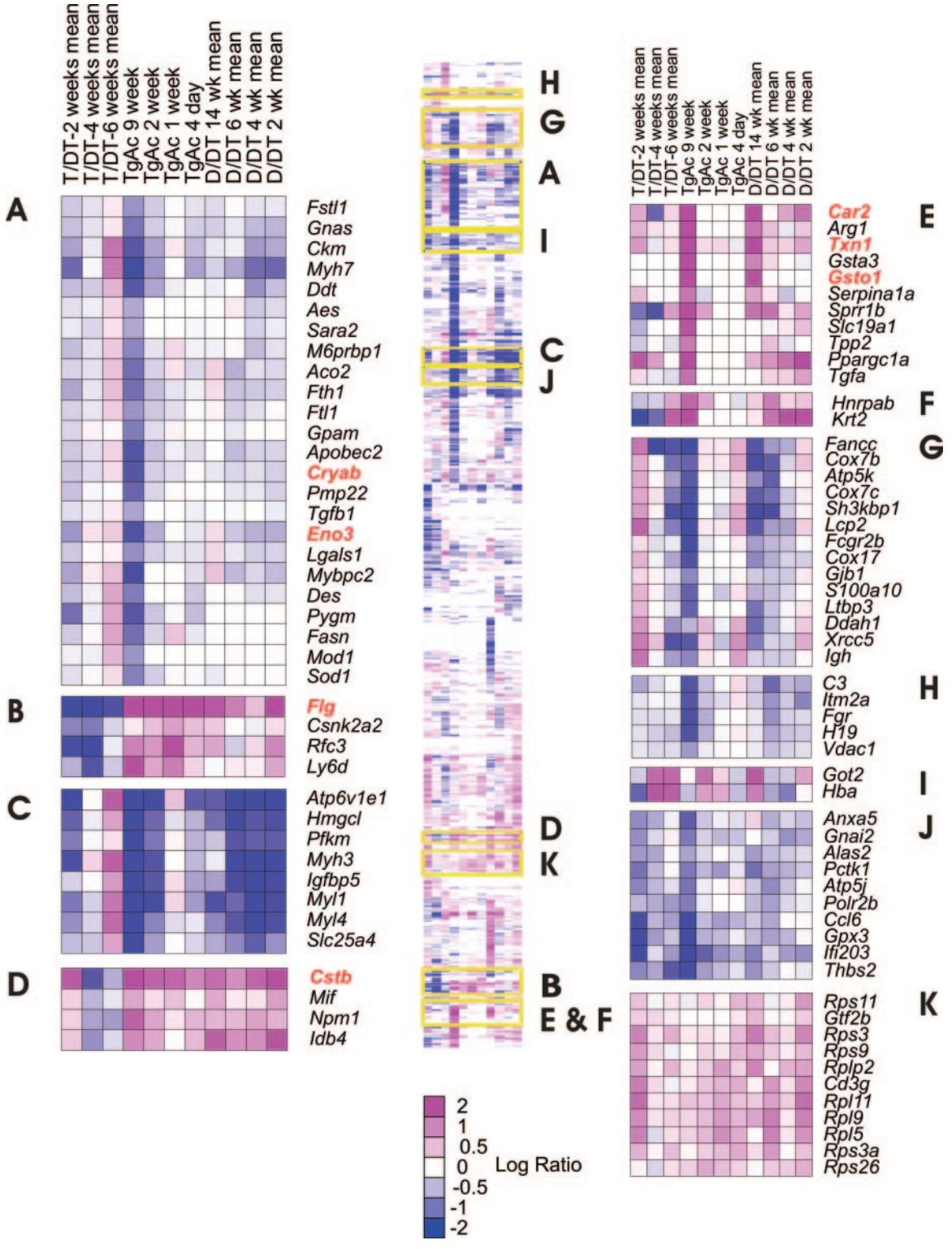

Fig. 3. Cluster analysis of promotion and tumor-associated gene expression. FVB/N mice were treated with DMBA (10 μg) 1 week prior to commencing TPA or acetone vehicle control treatment (DT or D, respectively). Control FVB/N mice that received acetone instead of DMBA were also treated with TPA (T). Tg.Ac mice were treated with TPA or acetone vehicle control for the indicated times. Microarray comparisons were carried out between FVB/N D/DT and T/DT. Tg.Ac sample comparisons were made between acetone and TPA-treated skins, indicated just as Tg.Ac. All genes that were significantly altered ($P \leq 0.05$) in expression in at least one sample were clustered using hierarchical clustering (GeneCluster 3.0). The central panel shows a treeview visualization (either MapleTree (0.2.3.2 Beta or treeview 1.5 (http://rana.lbl.gov/EisenSoftware.htm). The highest density of colour is associated with a 4-fold ($\log_2$=2) or more differential regulation, mauve is upregulated and blue downregulated with respect to the ratio as shown in the header or in the case of Tg.Ac animals it is the TPA-treated over the control (acetone-treated). Clusters associated with differentiation, associated as described in the text, are shown in panels A–D with those primarily downregulated in response to differentiation in panels A and C, and those upregulated in panels B and D. Differential gene expression associated more with tumor and tumor formation, associated as described in the text, is shown in panels E–K.
Panels E, F and I are genes increased in expression in response to tumor formation and those in panels G, H and J are downregulated. Panel K shows genes biochemically associated with increased translation in response to the tumor process. Gene symbols are associated with names in Table II.

most interpretable data. The clustering of the whole 617 genes is shown in Figure 3 and from this individual clusters were selected based on the pathological criterion. The clusters in Figures 3A–D show genes whose differential expression was primarily associated with differentiation. The criterion for this selection was an inverse gene expression response in the T/DT experiments compared with the Tg.Ac and D/DT experiments. The reason was that the differentiation response to TPA was partially inhibited by DMBA indicated by the decreased *Involucrin* (Figure 2M) and *Filaggrin* (Figure 3B) expression. Figures 3E–J show gene clusters associated with carcinogenesis. The primary criterion for selection of these genes was a similar alteration in expression in the tumor-bearing 9 week Tg.Ac and 14 week D/DT samples. Additionally, it was decided that the genes selected here should not be differentially expressed to the same degree in the earlier time point samples, where tumor formation had not occurred and should not show an inverse expression in the T/DT sample. This can be seen particularly for the genes *Gsto1, Txn1* and *Car2* in cluster E. We were confident with the association of cluster E with tumorigenesis as *Txn1* overexpression has been shown to induce papillomas in mice (21). Cluster E shows upregulated genes as do F and I; though in F the response in the 14 week D/DT samples is less marked than that in the 9 week Tg.Ac and in cluster I the converse. Clusters G, H and J show downregulated genes. The downregulated genes shown in clusters H and J were though not equivalent in the 9 week Tg.Ac and 14 week D/DT samples as they were in cluster G. This may have been due to sample selection or not exact matching of the stage of tumorigenesis between the two models. Cluster K is differentiated from the others in this group by time. The alterations in gene expression through the three samples are similar indicating that these are associated with tumor formation rather than other pathological changes in the skin. However, the responses are occurring very early in the time course and decreasing in the tumor-bearing samples (9 week Tg.Ac and 14 week D/DT). This strongly suggests a differential gene expression in response to a change in biochemical homeostasis. Many of the genes in this cluster are ribosomal. It is therefore feasible that translation is changing in the skin which could be related to the synthesis of proteins for proliferation, differentiation and tumor formation. EASE analysis confirmed this hypothesis (Table I) showing a strong correlation of genes associated with protein biosynthesis with the proliferation.

Table I. EASE analysis of the differentiation and proliferation-associated genes

Gene category	EASE score differentiation	EASE score proliferation
Muscle contraction	0.004899056	Not found
Morphogenesis	0.007498614	0.999919778
Organogenesis	0.007498614	0.999919778
Development	0.007763048	0.999818149
Muscle fibre	0.012455008	Not found
Energy derivation by oxidation of organic compounds	0.017112388	Not found
Cell motility	0.029705815	1
Muscle development	0.029705815	1
Myosin	0.044608603	Not found
Structural constituent of muscle	0.056195051	Not found
Protein metabolism	0.056195051	0.000918269
Structural constituent of ribosome	Not found	0.002213819
Protein biosynthesis	Not found	0.002213819
Ribonucleoprotein complex	Not found	0.003698428
Ribosome	Not found	0.003698428
Macromolecule biosynthesis	1	0.008999639
Biosynthesis	0.999893738	0.009918753
Cytosolic ribosome (sensu Eukarya)	Not found	0.020030629
Nucleic acid binding	0.99896311	0.034868438
RNA binding	0.999478122	0.039342737

This table shows the EASE analysis of the differentiation (upper set) and proliferation-associated (lower set) of genes. The gene sets compared were those shown in Figure 3 panels A–D against those in panels E–K. Bootstrapping was performed with 10 000 iterations and the sets with an EASE score of less than 0.05 are shown. For clarity the actual gene annotations in each set have been left out of the table.

RT–PCR confirmation of microarray findings

Genes indicated in red on Figure 3 were representative for a given cluster and their expression changes confirmed by RT–PCR. In Figure 4A, RT–PCR verification of differential gene expression is shown for seven genes from the differentiation-associated (patterned bars) and carcinogenesis (solid bars) associated sets. Verification was performed at two time points, for the FVB/N mouse experiment weeks 2 and 14, and also week 9 and dissected tumor from the Tg.Ac mice. Although the time points were selected on the basis of no papilloma formation; proliferation and differentiation had occurred during week 2 and papilloma formation during week 14 FVB/N and week 9 Tg.Ac. The tissue used from the week 14 FVB/N and week 9 Tg.Ac mice contained both papillomas and surrounding skin. Those genes which were assigned as differentiation-associated *Eno3*, *Cstb*, *Flg* and *Cryab* (Figure 4A patterned bars) were differentially expressed to approximately the same degree in week 2 and the tumor-bearing skin. In comparison, differential expression of the tumor-associated genes *Txn1*, *Car2* and *Gsto1* (Figure 4A solid bars) was very much greater in the tumor samples justifying their designation as being more associated with the tumor formation than proliferation or differentiation. One gene that was particularly well associated with tumorigenesis was *Gsto1*. This gene was therefore chosen for following through the time course for both the FVB/N (Figure 4B solid bars) and Tg.Ac experiments (Figure 4B striped bars). In both FVBN and Tg.Ac, the differential expression of this gene was much greater in the tumor-bearing samples (black) compared with the earlier time point samples from each experiment (grey). For the FVB/N samples TPA-treated skin was used for comparison to normalize for any effects of differentiation.

In situ analysis

The location of *Gsto1* in the papillomas was determined using *in situ* analysis (Figures 5A and B) and compared with the localization in untreated skin (Figure 5C). Expression was predominant in the proliferating area of the papillomas. In the normal skin some expression was detectable in the suprabasal layers (Figure 5C). At higher power, expression could be seen it in the upper hair follicles (Figure 5D).

EASE analysis

To discern if there were any particular gene classes that were significantly associated with the process of proliferation or differentiation the genes associated in Figure 3 with these processes were submitted for analysis using EASE (18). The predominant classes associated with each set of genes are shown in Table I. The main class of genes associated with the skin differentiation were members of the myosin

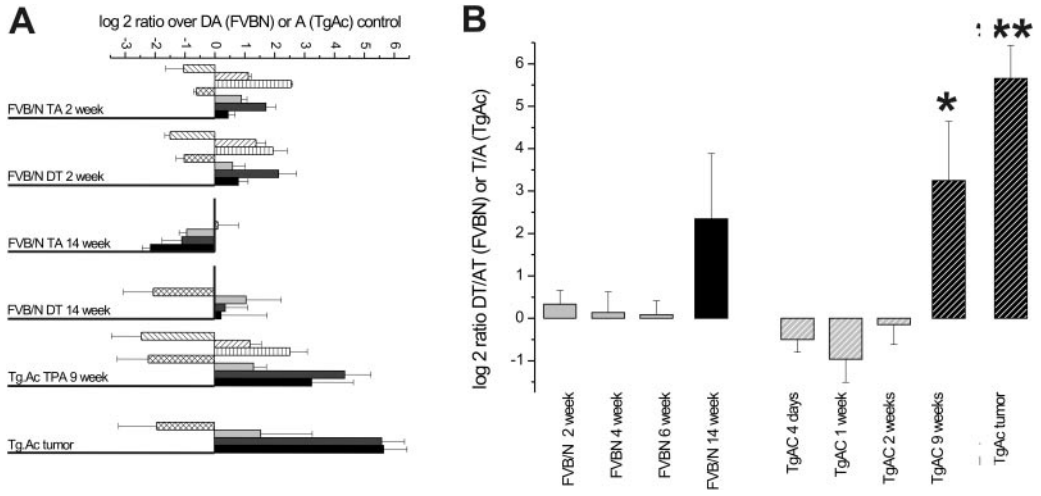

Fig. 4. Confirmation of promotion-associated gene expression changes by RT–PCR. The level of gene expression of selected TPA-associated genes in the mouse samples was confirmed by RT–PCR. (**A**) For each experimental comparison, the genes more associated with promotion are in the patterned bars, and those with tumor formation, in the solid bars. In each plot the bars represent the genes as follows (left to right). Differentiation-associated: forward slash; *Eno3*, back slash; *Cstb*, horizontal line; *Flg*, Cross hatch *Cryab*. Tumor-associated: light grey; *Txn1*, dark grey; *Car2*, black; *Gsto1*. The mouse strains and time points are shown in the figure. The comparisons are all against an initiated only control (D) or for Tg.Ac an acetone-treated control. T mice are promoted only and DT mice, initiated and promoted. Tumors occurred in the DT 14 week sample and Tg.Ac 9 week sample. The Tg.Ac tumor is a dissected tumor sample. (**B**) *Gsto1* expression through the FVB/N (solid bars) and Tg.Ac (striped bars) time course. FVB/N samples are a ratio of expression in the DT (tumor forming) samples over T (proliferation) or the Tg.Ac-promoted mouse (T) against the acetone control (A). The final bar is a dissected tumor from a 9 week Tg.Ac-promoted mouse. Experiments associated where tumor formation has not occurred are in light grey and those samples where tumor formation has occurred are in black. Ratios are derived from the division of the average of three independent experimental determinations and converted to $\log_2$ for clarity of presentation. $^{*}P \leq 0.05$; $^{**}P \leq 0.01$ are two-tailed unpaired Student's *t*-test results.

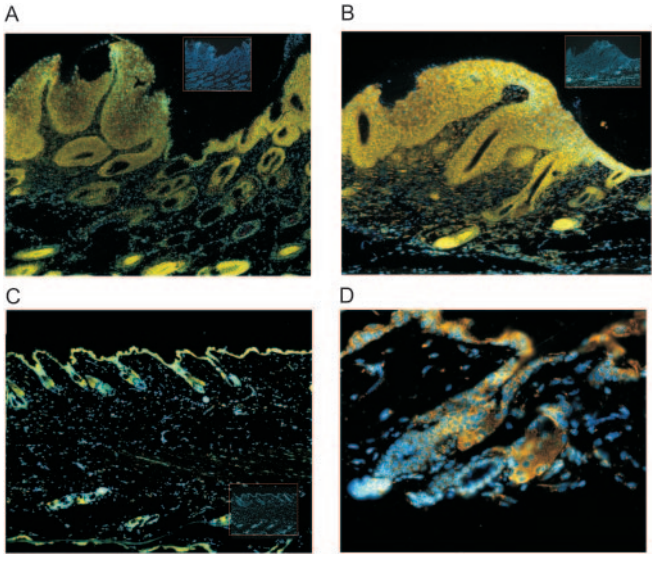

Fig. 5. *In situ* hybridization to localize the expression of the *gsto1* in the papillomas. Panels A and B are both papillomas from TPA-treated TgAc mice. The yellow fluorescence indicates the presence of the *gsto1* mRNA and the nuclei are counterstained in Hoechst 33342. Panels C and D are from an untreated mouse skin. Inset panels show the no probe negative controls stained with Hoechst 33342.

family which are generally associated with muscle development (*mybpc2*, *myh7* (Figure 3A), *myh3*, *myl1* and *myl4* (Figure 3C)). For the proliferation-associated genes (Figure 3), the main gene association was with the classes of genes linked by a functional association with protein synthesis. As we had defined these genes as being associated with proliferation, it was not altogether surprising to find that these were the main classes of genes overrepresented. Of the three genes that were particularly characterized, *Gsto1* in downstream analysis has not been previously associated with proliferation and tumorigenesis in the skin.

Discussion

FVB/N and Tg.Ac mice are established mouse models widely used to study skin carcinogenesis. This investigation was undertaken to identify genes whose differential expression was more closely associated with the pathological phases of keratinocyte proliferation, differentiation and papilloma formation. Though association of these cannot be absolute as tumor tissue is by definition proliferating, it was possible to identify gene clusters more closely associated with each pathological phase. In particular, the genes associated with the tumor formation were more evident. It is theoretically possible that the differential gene expression observed could be due to inflammatory infiltrate. However, little inflammation was observed pathologically or indicated by the differential gene expression. It seems more likely therefore that the differential gene expressions measured here reflect changes in the keratinocytes. Initiated and promoted FVB/N and promoted Tg.Ac mice responded as expected to the dosing regimes employed (Figure 1). The average number of papillomas per mouse and latency time to first papilloma appearance in the Tg.Ac mice were comparable with results reported previously (22). The FVB/N mice in this study showed a comparable papilloma burden to that reported by Battalora (13) using a similar treatment schedule (Figure 1). Epidermal proliferation and differentiation was present in all mice that had been promoted irrespective of initiation and was evident as early as 2 weeks after the start of promotion as has been reported previously (23) (Figure 2B). However, differentiation was

Table II. Gene annotation for the HUGO annotated genes shown in Figure 3

A.	Fstl1	Follistatin-like 1
	Gnas	Guanine nucleotide binding protein, alpha stimulating complex locus
	Ckm	Creatine kinase, muscle
	Myh7	Myosin, heavy polypeptide 7, cardiac muscle, beta
	Ddt	D-dopachrome tautomerase
	Aes	Amino-terminal enhancer of split
	Sara2	SAR1a gene homologue 2 (*S. cerevisiae*)
	M6prbp1	Mannose-6-phosphate receptor binding protein 1
	Aco2	Aconitase 2, mitochondrial
	Fth1	Ferritin heavy chain 1
	Flt1	fms-related tyrosine kinase 1 (vascular endothelial growth factor/vascular permeability factor receptor)
	Gpam	Glycerol-3-phosphate acyltransferase, mitochondrial
	Apobec2	Apolipoprotein B editing complex 2
	Cryab	Crystallin, alpha B,
	Pmp22	Peripheral myelin protein
	Tgfb1	Transforming growth factor
	Eno3	Enolase 3, beta muscle
	Lgals1	Lectin, galactose binding, soluble 1
	Mybpc2	Myosin binding protein C
	Des	Desmin
	Pygm	Muscle glycogen phosphorylase
	Fasn	Fatty acid synthase
	Mod1	Malic enzyme, supernatant
	Sod1	Superoxide dismutase 1
B.	Flg	Filaggrin
	Csnk2a2	Casein kinase II
	Rfc3	Replication factor C (activator 1) 3
	Ly6d	Lymphocyte antigen 6 complex
C.	Atp6v1e1	ATPase, H+ transporting, lysosomal 31kDa, V1 subunit E isoform 1
	Hmgcl	3-Hydroxy-3-methylglutaryl-coenzyme A lyase
	Pfkm	Phosphofructokinase, muscle
	Myh3	Myosin, heavy polypeptide 3
	Igfbp5	Insulin-like growth factor binding protein 5
	Myl1	Myosin, light polypeptide 1
	Myl4	Myosin, light polypeptide 4
	Slc25a4	Solute carrier family 25
D.	Cstb	Cystatin B
	Mif	Macrophage migration inhibitory factor
	Npm1	Nucleophosmin
	Idb4	Inhibitor of DNA binding 4
E.	Car2	Carbonic anhydrase 2
	Arg1	Arginase
	Txn1	Thioredoxin
	Gsta3	Glutathione S-transferase, alpha 3
	Gsto1	Glutathione S-transferase omega 1
	Serpina1a	Cell division cycle 2 homologue A
	Sprr1b	Small proline-rich protein 1B (cornifin)
	Slc19a1	Solute carrier family 19 (folate transporter), member 1
	Tpp2	Tripeptidyl peptidase II
	Ppargc1a	Peroxisome proliferative activated receptor
	Tgfa	Transforming growth factor alpha
F.	Hnrpab	Heterogeneous nuclear ribonucleoprotein A/B
	Krt2	Keratin
G.	Fancc	Fanconi anaemia, complementation group C
	Cox7b	Cytochrome c oxidase subunit VIIb
	Atp5k	ATP synthase, H+ transporting, mitochondrial F1F0 complex, subunit e
	Cox7c	Cytochrome c oxidase, subunit VIIc
	Sh3kbp1	SH3-domain kinase binding protein 1
	Lcp2	Lymphocyte cytosolic protein 2
	Fcgr2b	Fc receptor, IgG
	Cox17	COX17 homologue, cytochrome c oxidase assembly protein
	Gjb1	Gap junction membrane channel protein beta 1
	S100a10	S100 calcium binding protein A10 (calpactin)
	Ltbp3	Latent transforming growth factor beta binding protein 3
	Ddah1	Dimethylarginine dimethylaminohydrolase 1
	Xrcc5	X-ray repair complementing defective repair in Chinese hamster cells 5
	Igh	AT rich interactive domain 3A
H.	C3	Complement component 3
	Itm2a	Integral membrane protein 2A
	Fgr	Gardner-Rasheed feline sarcoma viral oncogene homologue
	H19	H19 fetal liver mRNA
	Vdac1	Voltage-dependent anion channel 1
I.	Got2	Glutamate oxaloacetate transaminase 2, mitochondrial
	Hba	Haemoglobin alpha chain
J.	Anxa5	Annexin A5
	Gnai2	Guanine nucleotide binding protein, alpha inhibiting 2
	Alas2	Aminolevulinic acid synthase 2, erythroid
	Pctk1	PCTAIRE-motif protein kinase 1
	Atp5j	ATP synthase, H+ transporting, mitochondrial F0 complex
	Polr2b	Polymerase (RNA) II (DNA directed) polypeptide B
	Ccl6	Chemokine (C-C motif) ligand 6
	Gpx3	Glutathione peroxidase 3
	Ifi203	Interferon inducible protein 203
	Thbs2	Thrombospondin 2
K.	Rps11	Ribosomal protein S11
	Gtf2b	General transcription factor IIB
	Rps3	Ribosomal protein S3
	Rps9	Ribosomal protein S9,
	Rplp2	Ribosomal protein, large P2
	Cd3g	CD3 antigen, gamma polypeptide,
	Rpl11	Ribosomal protein L11
	Rpl9	Ribosomal protein L9
	Rpl5	Ribosomal protein L5
	Rps3a	Ribosomal protein S3a
	Rps26	Ribosomal protein S26

For clarity only the HUGO gene symbols have been shown in Figure 3. The complete gene name is given here in the same order as Figure 3.

enhanced in TPA-treated skin compared with DMBA- and TPA-treated skin, and was manifest by the appearance of flattened cells containing prominent keratohyaline granules, and a marked induction of *Involucrin* and *Filaggrin* gene expression (24). This response was not unexpected as initiated cells are known to escape differentiation.

Differentiation-associated genes

Those genes identified as being changed in expression in a manner associated with differentiation were generally altered at early time points and remained differentially expressed through to tumorigenesis (Figure 3A–D). The altered expression of *Eno3*, *Cstb* and *Flg* have previously been recorded in response to differentiation induced by TPA (12,25–28). A decrease in *Eno3* expression has been demonstrated in mouse skin 6 h after TPA treatment (12). *Eno3* was consistently reduced in expression throughout the time course of this study, and was classified as a proliferation and differentiation responsive gene (Figure 3A and 4A). *Eno3* is the muscle-specific form of enolase, associated with glycolysis and inherited recessive metabolic myopathy in humans (29). Therefore, decreased expression of *Eno3* may be associated with its role in glycolysis, and potentially suggests a reduced requirement for energy in the differentiating skin. EASE analysis demonstrated an interesting correlation though of skin differentiation with the expression of muscle-specific genes (Table I) in particular members of the myosin family and *Eno3*. There has been a previous association of myosin expression with dermatofibromas and it could be that the smooth muscle proteins are specific markers for differentiating as opposed to proliferative skin lesions (30).

Both *Cstb* and *Flg* are associated with keratinocyte differentiation and found in the cornified envelope (25–28). Commensurate with this *Flg* is also known to be increased during calcium-induced differentiation of skin cells (26,28) and in response to TPA and v-ras transfection. Homologues of *Cstb* have been demonstrated to be crosslinked to *Flg* by transglutaminase, a process that occurs in cornified envelope formation. *Cstb* homologues are also elevated in expression during wound healing (11,31). Thus, the alteration in expression of these two genes with differentiation and proliferation as seen in this study is entirely consistent with the known functional roles for these genes in skin. Reduced expression of the chaperone protein *Cryab* was consistent in both strains of mice across the time course studied (Figure 3A and 4A). The elevation of *Cryab* expression has been associated with resistance to the effects of DNA-damaging drugs (32), and reduced *Cryab* expression in epithelial ovarian cancer correlates with reduced median survival time (33).

Tumor and proliferation-associated genes

Tumor and proliferation-associated genes were primarily defined by their differential expression in the tumor-bearing skin samples and are shown in Figure 3 (E–K). EASE analysis of this gene set (Table I) primarily identified genes associated with protein synthesis. Given that these genes had been selected on the basis of their differential expression in tumor-bearing samples; this is perhaps not a surprising association. For further analysis we chose three genes whose differential expression was strongly associated with tumor formation, but were not included in the EASE analysis of genes associated with protein synthesis. Increased expression of the tumor-associated gene *Txn1* was small (Figure 3E) when assessed by microarray analysis. We chose to investigate this gene further because of its known cancer association. Using RT–PCR we further corroborated significant changes in the expression of *Txn1* in 9 weeks promoted Tg.Ac skin. DMBA and TPA have previously been demonstrated to increase the activity of *Txn1* (34). Thus, it may be that *Txn1* induction is partly modulated by both proliferation/differentiation and cancer-associated mechanisms. *Txn1* was elevated in the three samples containing papillomas that were analysed by RT–PCR (Figure 4A). There are conflicting reports on the effect of *Txn1* expression on cell growth. Recombinant Txn enhances the growth of NIH3T3 cells, whereas in HeLa, *Txn1* is required for interferon γ-mediated growth inhibition (35,36). In mice, a 2-fold overexpression of *Txn1* leads to an increase in papilloma formation with the DT protocol (21). Immunostaining has shown *Txn1* in differentiated squamous cell carcinomas (37) and expression has been found to be increased in gastric carcinomas (38).

Car2 and *Gsto1* gene expression was markedly increased in expression during the course of these studies, as demonstrated both by microarray analysis and RT–PCR. The mRNA levels of *Car2* were altered in both a promotion-dependent (early time points) and a skin papilloma-associated manner. The possibility of a *Car2* role in skin cell differentiation in response to TPA promotion is appealing as *Car2* is present in differentiated osteoclasts. It is induced by differentiation stimuli and inhibited when terminal differentiation is abrogated (39–41). However, here the changes in *Car2* levels were associated with papilloma formation (Figure 4A), and therefore the control stimuli may be different. Strongly associated with the formation of the skin tumors was increased expression of *Gsto1* (Figures 3E, 4A and B). *In situ* analysis clearly showed the expression of this gene within the proliferative areas of the papillomas (Figure 5A and B). Although *Gsto1* is classified as a Gst, this isoform not only has weak Gst activity, but also possesses other thiol transferase (42) and dehydroascorbate reductase (43) activities more widely associated with glutaredoxins. Dehydroascorbate reductase activity may be pertinent to the skin as several *in vitro* studies have shown that ascorbate or its stable derivative AA-2P cause keratinocyte cell differentiation, protect against UV-induced cell damage and enhance production of lipids associated with the cornified envelope (44–46). In a survey of human tissues, *Gsto1* was only found expressed within the macrophages of the skin (47). However, it is unlikely that macrophages are solely responsible for the *Gsto1* detected within the skin in this study, as we did not see an inflammatory infiltrate either within papillomas or hyperplastic skin. *Gstpi*, another member of the GST family has been shown to function as a tumor suppressor in skin carcinogenesis experiments and *Gstpi* null mice show enhanced sensitivity to chemically induced skin tumorigenesis (48). We did not see increased expression of *Gstpi*, though there was an increased expression of *Gsta1*, which showed a similar expression profile to that of *Gsto1*.

Generally increased in expression through the time course to tumor formation in all comparisons were members of the ribosomal family such as *Rpl11*. The increased expression of these genes would indicate a general increase in translation and protein synthesis. These genes were primary contributors to the EASE identification of gene classes associated with protein synthesis (Table I). Previously there have been reports of increased translation in response to TPA, e.g. of the elongation factors, and this would not be unexpected; given the proliferation response and the increased need for protein (49).

In summary, this work has identified some genes differentially expressed and associated with the general effects of tumor promotion and differentiation in the skin, and others more closely associated with papilloma formation in FVB/N and Tg.Ac mice. Some of these were altered prior to the formation of papillomas and were associated with papilloma formation. The association of *Gsto1*, *Cryab* and *Car2* with tumor formation suggests a potentially fundamental role for these proteins in the process of tumor formation and development.

Acknowledgements

The authors would like to acknowledge, David J Judah, Jin Li Luo and Joan Riley for the preparation of microarrays and bioinformatics assistance. We would also like to thank Jenny Edwards and Linda Wilkinson for pathology support and are grateful to Colin Travis and the Division of Biomedical Sciences for assistance with the animal experiments. We thank Dr P Carthew for his advice and interest. This study was supported and funded by the European Chemical Industry Council Long Range Initiative (CEFIC-LRI). Funding to pay the Open Access publication charges for this article was provided by CEFIC-LRI.

Conflict of Interest Statement: None declared.

References

1. DiGiovanni,J., Slaga,T.J. and Boutwell,R.K. (1980) Comparison of the tumor-initiating activity of 7,12-dimethylbenz[a]anthracene and benzo[a]pyrene in female SENCAR and CS-1 mice. *Carcinogenesis*, **1**, 381–389.

2. Hennings,H., Devor,D., Wenk,M.L., Slaga,T.J., Former,B., Colburn,N.H., Bowden,G.T., Elgjo,K. and Yuspa,S.H. (1981) Comparison of 2-stage epidermal carcinogenesis initiated by 7,12-dimethylbenz(a)anthracene or N-methyl-N′-nitro-N- nitrosoguanidine in newborn and adult sencar and balb-C mice. *Cancer Res.*, **41**, 773–779.
3. Leder,A., Kuo,A., Cardiff,R.D., Sinn,E. and Leder,P. (1990) V-Ha-Ras transgene abrogates the initiation step in mouse skin tumorigenesis—effects of phorbol esters and retinoic acid. *Proc. Natl Acad. Sci. USA*, **87**, 9178–9182.
4. Binder,R.L., Gallagher,P.M., Johnson,G.R., Stockman,S.L., Smith,B.J., Sundberg,J.P. and Conti,C.J. (1997) Evidence that initiated keratinocytes clonally expand into multiple existing hair follicles during papilloma histogenesis in SENCAR mouse skin. *Mol. Carcinog.*, **20**, 151–158.
5. Binder,R.L., Johnson,G.R., Gallagher,P.M., Stockman,S.L., Sundberg,J.P. and Conti,C.J. (1998) Squamous cell hyperplastic foci: precursors of cutaneous papillomas induced in SENCAR mice by a two-stage carcinogenesis regimen. *Cancer Res.*, **58**, 4314–4323.
6. Dlugosz,A.A. and Yuspa,S.H. (1993) Coordinate changes in gene-expression which mark the spinous to granular-cell transition in epidermis are regulated by protein- kinase-C. *J. Cell Biol.*, **120**, 217–225.
7. Wei,S.J., Trempus,C.S., Cannon,R.E., Bortner,C.D. and Tennant,R.W. (2003) Identification of Dss1 as a 12-O-tetradecanoylphorbol-13-acetate-responsive gene expressed in keratinocyte progenitor cells, with possible involvement in early skin tumorigenesis. *J. Biol. Chem.*, **278**, 1758–1768.
8. Wei,S.J., Trempus,C.S., Ali,R.C., Hansen,L.A. and Tennant,R.W. (2004) 12-O-tetradecanoylphorbol-13-acetate and UV radiation-induced nucleoside diphosphate protein kinase B mediates neoplastic transformation of epidermal cells. *J. Biol. Chem.*, **279**, 5993–6004.
9. Gariboldi,M., Peissel,B., Fabbri,A. *et al.* (2003) SCCA2-like serpins mediate genetic predisposition to skin tumors. *Cancer Res.*, **63**, 1871–1875.
10. Sesto,A., Navarro,M., Burslem,F. and Jorcano,J.L. (2002) Analysis of the ultraviolet B response in primary human keratinocytes using oligonucleotide microarrays. *Proc. Natl Acad. Sci. USA*, **99**, 2965–2970.
11. Pedersen,T.X., Leethanakul,C., Patel,V., Mitola,D., Lund,L.R., Dano,K., Johnsen,M., Gutkind,J.S. and Bugge,T.H. (2003) Laser capture microdissection-based in vivo genomic profiling of wound keratinocytes identifies similarities and differences to squamous cell carcinoma. *Oncogene*, **22**, 3964–3976.
12. Schlingemann,J., Hess,J., Wrobel,G. *et al.* (2003) Profile of gene expression induced by the tumor promotor TPA in murine epithelial cells. *Int. J. Cancer*, **104**, 699–708.
13. Battalora,M.S., Spalding,J.W., Szczesniak,C.J., Cape,J.E., Morris,R.J., Trempus,C.S., Bortner,C.D., Lee,B.M. and Tennant,R.W. (2001) Age-dependent skin tumorigenesis and transgene expression in the Tg.AC (v-Ha-ras) transgenic mouse. *Carcinogenesis*, **22**, 651–659.
14. Diehel,F., Grahlmann,S., Beier,M. and Hoheisel,J. (2001) Manufacturing DNA microarrays of high spot homogeneity and reduced background signal. *Nucleic Acids Res.*, **29**, e38.
15. Turton,N.J., Judah,D.J., Riley,J., Davies,R., Lipson,D., Styles,J.A., Smith,A.G. and Gant,T.W. (2001) Gene expression and amplification in breast carcinoma cells with intrinsic and acquired doxorubicin resistance. *Oncogene*, **20**, 1300–1306.
16. Hegde,P., Qi,R., Abernathy,K., Gay,C., Dharap,S., Gaspard,R., Hughes,J.E., Snesrud,E., Lee,N. and Quackenbush,J. (2000) A concise guide to cDNA microarray analysis. *Biotechniques*, **29**, 548–550.
17. Zhang,S.D. and Gant,T.W. (2004) A statistical framework for the design of microarray experiments and effective detection of differential gene expression. *Bioinformatics*, **20**, 2821–2828.
18. Hosack,D., Dennis,G.J., Sherman,B., Land,H. and Lempicki,R. (2003) Identifying biological themes within lists of genes with EASE. *Genome Biol.*, **4**, R70.
19. Eckert,R., Crish,J., Efimova,T., Dashti,S., Deucher,A., Bone,F., Adhikary,G., Huang,G., Gopalakrishnan,R. and Balasubramanian,S. (2004) Regulation of involucrin gene expression. *J. Invest. Dermatol.*, **123**, 13–22.
20. Candi,E., Schmidt,R. and Merlino,G. (2005) The cornified envelope: a model of cell death in the skin. *Nat. Rev. Mol. Cell Biol.*, **4**, 328–340.
21. Mustacich,D., Wagner,A., Williams,R., Bair,W., Barbercheck,L., Stratton,S., Bhattacharyya,A. and Powis,G. (2004) Increased skin carcinogenesis in a keratinocyte directed thioredoxin-1 transgenic mouse. *Carcinogenesis*, **10**, 1983–1989.
22. Trempus,C.S., Bishop,W.R., Njoroge,F.G., Boll,R.J., Battalora,M.S., Mahler,J.G., Haseman,J.K. and Tennant,R.W. (2000) A farnesyl transferase inhibitor suppresses TPA-mediated skin tumor development without altering hyperplasia in the ras transgenic Tg.AC mouse. *Mol. Carcinog.*, **27**, 24–33.
23. Hansen,L.A. and Tennant,R. (1994) Focal transgene expression associated with papilloma development in V-Ha-Ras-transgenic Tg.Ac mice. *Mol. Carcinog.*, **9**, 143–154.
24. Marcelo,C.L. and Tong,P.S.L. (1983) Epidermal keratinocyte growth: changes in protein composition and synthesis of keratins in differentiating cultures. *J. Invest. Dermatol.*, **80**, 37–44.
25. Steven,A.C. and Steinert,P.M. (1994) Protein-composition of cornified cell envelopes of epidermal- keratinocytes. *J. Cell Sci.*, **107**, 693–700.
26. Li,L.W., Tucker,R.W., Hennings,H. and Yuspa,S.H. (1995) Inhibitors of the intracellular Ca2+-atpase in cultured mouse keratinocytes reveal components of terminal differentiation that are regulated by distinct intracellular Ca2+ compartments. *Cell Growth Differ.*, **6**, 1171–1184.
27. Stanwell,C., Dlugosz,A.A. and Yuspa,S.H. (1996) Staurosporine induces a complete program of terminal differentiation in neoplastic mouse keratinocytes via activation of protein kinase C. *Carcinogenesis*, **17**, 1259–1265.
28. Elias,P.M., Ahn,S.K., Denda,M., Brown,B.E., Crumrine,D., Kimutai,L.K., Komuves,L., Lee,S.H. and Feingold,K.R. (2002) Modulations in epidermal calcium regulate the expression of differentiation-specific markers. *J. Invest. Dermatol.*, **119**, 1128–1136.
29. Comi,G.P., Fortunato,F., Lucchiari,S. *et al.* (2001) Beta-enolase deficiency, a new metabolic myopathy of distal glycolysis. *Ann. Neurol.*, **50**, 202–207.
30. Bruecks,A. and Trotter,M. (2002) Expression of desmin and smooth muscle myosin heavy chain in dermatofibromas. *Arch. Pathol. Lab. Med.*, **126**, 1179–1183.
31. Takahashi,M., Tezuka,T., Kakegawa,H. and Katunuma,N. (1994) Linkage between phosphorylated cystatin a and filaggrin by epidermal transglutaminase as a model of cornified envelope and inhibition of cathepsin-L activity by cornified envelope and the conjugated cystatin-alpha. *FEBS Lett.*, **340**, 173–176.
32. Wittig,R., Nessling,M., Will,R.D., Mollenhauer,J. *et al.* (2002) Candidate genes for cross-resistance against DNA-damaging drugs. *Cancer Res.*, **62**, 6698–6705.
33. Stronach,E.A., Sellar,G.C., Blenkiron,C. *et al.* (2003) Identification of clinically relevant genes on chromosome 11 in a functional model of ovarian cancer tumor suppression. *Cancer Res.*, **63**, 8648–8655.
34. Kumar,S. and Holmgren,A. (1999) Induction of thioredoxin, thioredoxin reductase and glutaredoxin activity in mouse skin by TPA, a calcium ionophore and other tumor promoters. *Carcinogenesis*, **20**, 1761–1767.
35. Oblong,J.E., Berggren,M., Gasdaska,P.Y., Hill,S.R. and Powis,G. (1995) Site-Directed mutagenesis of Lys(36) in human thioredoxin—the highly conserved residue affects reduction rates and growth-stimulation but is not essential for the redox proteins biochemical or biological properties. *Biochemistry*, **34**, 3319–3324.
36. Deiss,L.P. and Kimchi,A. (1991) A genetic tool used to identify thioredoxin as a mediator of a growth inhibitory signal. *Science*, **252**, 117–120.
37. Wakita,H., Yodoi,J., Masutani,H., Toda,K. and Takigawa,M. (1992) Immunohistochemical distribution of adult t-cell leukemia- derived factor thioredoxin in epithelial components of normal and pathological human skin conditions. *J. Invest. Dermatol.*, **99**, 101–107.
38. Grogan,T.M., Fenoglio-Prieser,C., Zeheb,R. *et al.* (2000) Thioredoxin, a putative oncogene product, is overexpressed in gastric carcinoma and associated with increased proliferation and increased cell survival. *Human Pathol.*, **31**, 475–481.
39. Lomri,A. and Baron,R. (1992) 1-alpha-25-dihydroxyvitamin-D3 regulates the transcription of carbonic anhydrase-Ii messenger-Rna in avian myelomonocytes. *Proc. Natl Acad. Sci. USA*, **89**, 4688–4692.
40. David,J.P., Rincon,M., Neff,L., Horne,W.C. and Baron,R. (2001) Carbonic anhydrase II is an AP-1 target gene in osteoclasts. *J. Cell. Physiol.*, **188**, 89–97.
41. Rietveld,L.E.G., Caldenhoven,E. and Stunnenberg,H.G. (2001) Avian erythroleukemia: a model for corepressor function in cancer. *Oncogene*, **20**, 3100–3109.
42. Board,P.G., Coggan,M., Chelvanayagam,G. *et al.* (2000) Identification, characterization, and crystal structure of the omega class glutathione transferases. *J. Biol. Chem.*, **275**, 24798–24806.
43. Ishikawa,T., Casini,A.F. and Nishikimi,M. (1998) Molecular cloning and functional expression of rat liver glutathione-dependent dehydroascorbate reductase. *J. Biol. Chem.*, **273**, 28708–28712.
44. Savini,I., Catani,V., Rossi,A., Duranti,G., Melino,G. and Avigliano,L. (2002) Characterization of keratinocyte differentiation induced by ascorbic acid: Protein kinase C involvement and vitamin C homeostasis. *J. Invest. Dermatol.*, **118**, 372–379.

45. Meves,A., Stock,S.N., Beyerle,A., Pittelkow,M.R. and Peus,D. (2002) Vitamin C derivative ascorbyl palmitate promotes ultraviolet-B-induced lipid peroxidation and cytotoxicity in keratinocytes. *J. Invest. Dermatol.*, **119**, 1103–1108.
46. Uchida,Y., Behne,M., Quiec,D., Elias,P.M. and Holleran,W.M. (2001) Vitamin C stimulates sphingolipid production and markers of barrier formation in submerged human keratinocyte cultures. *J. Invest. Dermatol.*, **117**, 1307–1313.
47. Yin,Z.L., Dahlstrom,J.E., Le Couteur,D.G. and Board,P.G. (2001) Immunohistochemistry of omega class glutathione S-transferase in human tissues. *J. Histochem. Cytochem.*, **49**, 983–987.
48. Henderson,C.J., Smith,A.G., Ure,J., Brown,K., Bacon,E.J. and Wolf,C.R. (1998) Increased skin tumorigenesis in mice lacking pi class glutathione S-transferases. *Proc. Natl Acad. Sci. USA*, **95**, 5275–5280.
49. Gschwendt,M., Kittstein,W. and Marks,F. (1988) Effect of tumor promoting phorbol ester TPA on epidermal protein synthesis: stimulation of an elongation factor 2 phosphatase activity by TPA in vivo. *Biochem Biophys Res Commun.*, **153**, 1129–1135.

Received July 25, 2005; revised February 11, 2006; accepted March 3, 2006